Subcutaneous Photovoltaic Infrared Energy Harvesting for Bio-implantable Devices

Eunseong Moon, *Student Member, IEEE*, David Blaauw, *Fellow, IEEE*, and Jamie D. Phillips, *Senior Member, IEEE*

***Abstract*— Wireless biomedical implantable devices on the millimeter-scale enable a wide range of applications for human health, safety, and identification, though energy harvesting and power generation are still looming challenges that impede their widespread application. Energy scavenging approaches to power biomedical implants have included thermal, kinetic, radio frequency, and radiative sources. However, the achievement of efficient energy scavenging for biomedical implants at the millimeter-scale has been elusive. Here, we show that photovoltaic cells at the millimeter-scale can achieve a power conversion efficiency of more than 17% for silicon and 31% for GaAs under 1.06 μW/mm^2 infrared irradiation at 850 nm. Finally, these photovoltaic cells demonstrate highly efficient energy harvesting through biological tissue from ambient sunlight, or irradiation from infrared sources such as used in present-day surveillance systems, by utilizing the near infrared transparency window between the 650- and 950-nm wavelength range.**

***Index Terms*— Energy harvesting, gallium arsenide, photovoltaics, silicon.**

I. Introduction

WIRELESS biomedical implantable devices are prospective technologies that can be applied to a variety of applications for monitoring physiological variables [18]–[21]. For these implantable applications, low-power systems on the millimeter-scale [22]–[26] with efficient energy harvesters from ambient and stable sources are essential to make these technologies practical. Several different energy sources utilizing thermal energy [1]–[3] and mechanical vibrations [4]–[6], and radio frequency (RF) electromagnetic radiation [7]–[11] have been evaluated and tested, though miniaturization and reliability/stability of the ambient sources are still primary limiting factors. Wireless power transfer via RF inductive coupling [7]–[11] is currently used in implantable systems today due to highly efficient power transfer around 58% at 13.56 MHz through the tissue with 250-mm^2 implanted coil area [10]. However, the power transfer efficiency is highly dependent on the distance between the primary and secondary coils [10], [11], decreasing power transfer efficiency exponentially from 58% with 1-cm distance to 0.16% with 5-cm distance [10] between coils. Efficiency also decreases dramatically as implantable device size decreases to millimeter-scale and below due to lateral and angular misalignments [27] and weak coupling [11] with millimeter-scale antenna receivers.

Biological tissue also provides a means of wireless power transfer in the near-infrared (NIR) spectral region, where there are two optical transparency windows in the 650–1350 nm range (First: 650–950 nm, Second: 1000–1350 nm) [15]–[17]. Photovoltaic cells can efficiently convert in this NIR spectral region [28], [29] with external quantum efficiency (EQE) approaching 100%, and are commonly utilized for high-efficiency solar cells. Photovoltaic cells for NIR subcutaneous energy harvesting face challenges in achieving high efficiency under low irradiance conditions in cells of small area, where shunt conductance [30]–[32] and perimeter recombination losses can dramatically degrade performance [30], [31]. Such cells are far more sensitive to shunt and recombination losses in comparison to solar cells that are typically centimeter-scale or larger and operating under irradiance that is orders of magnitude higher. Previous work on NIR photovoltaic infrared energy harvesting for biomedical implants [12]–[14], [33] utilized Photovoltaic (PV) cells on the centimeter-scale utilizing relatively high laser light irradiation (mw range), comparable to the intensity used for laser therapy treatments [34]. Here we demonstrate that photovoltaic cells at millimeter-scale can provide power densities needed for the perpetual operation of implantable devices via low-level irradiation at a wavelength of 850 nm in a through-tissue configuration.

II. Experiment

The NIR subcutaneous energy harvesting concept is illustrated in Fig. 1(a). Ambient outdoor sunlight or an external low-power infrared light source supplies power to the implanted device. Photovoltaic cells are based on materials, such as silicon or GaAs, which can efficiently convert the wavelength region in the NIR.

The PV cells may be stacked on the implantable system, and include an integrated photodiode to provide a means of low-power wireless optical communication to interface with the millimeter-scale system. We have studied both silicon and

Manuscript received January 24, 2017; revised March 8, 2017; accepted March 9, 2017. Date of publication March 27, 2017; date of current version April 19, 2017. This work was supported in part by the National Science Foundation and in part by the National Institutes of Health under Award R01CA195655. The review of this paper was arranged by Editor M. M. Hussain.

The authors are with the Department of Electrical Engineering and Computer Science, University of Michigan, Ann Arbor, MI 48109 USA (e-mail: esmoon@umich.edu; blaauw@umich.edu; jphilli@umich.edu).

Color versions of one or more of the figures in this paper are available online at http://ieeexplore.ieee.org.

Digital Object Identifier 10.1109/TED.2017.2681694

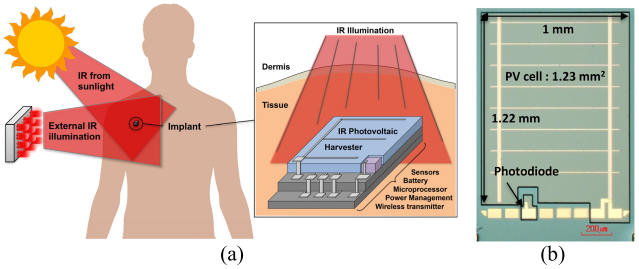

Fig. 1. (a) Conceptual illustration of subcutaneous photovoltaic energy harvesting through tissue. (b) Optical microscope image of a fabricated GaAs photovoltaic cells integrated with photodiode for wireless communication.

TABLE I
OPTIMIZED DEVICE PARAMETERS AT A WAVELENGTH BETWEEN 800 AND 850 NM

Material	Silicon		GaAs		
Parameter	Type	Value	Type	Value	Unit
Base thickness	p	35	n	2.75	μm
Base doping	p	2×10^{17}	n	10^{17}	cm^{-3}
Emitter thickness	n	0.34	p	0.5	μm
Emitter doping	n	2.5×10^{16}	p	4×10^{18}	cm^{-3}
Anti-reflection Si_3N_4 layer	-	100	-	100	nm

GaAs PV cells in this paper, where silicon offers advantages of compatibility with microelectronics technology, while GaAs offers superior light absorption properties, low dark current, and high shunt resistance. The silicon and GaAs PV cell designs were optimized for NIR illumination conditions using device simulations [30]. The optimized device parameters for silicon and GaAs PVs under low-flux NIR illumination between 800 and 850 nm are summarized in Table I. Fabricated cells utilized highly optimized surface passivation and anti-reflection layers to minimize perimeter recombination effects and the surface reflection at a wavelength of 800 nm; 50-nm low-pressure chemical vapor deposition Si_3N_4 + 50-nm plasma enhanced chemical vapor deposition (PECVD) Si_3N_4 for Silicon [30] and 100-nm PECVD $Si_3N_4$with $(NH_4)_2S$ surface treatment for GaAs.

Current–voltage characteristics of PV cells were measured utilizing Keithley 4200 and 2400 semiconductor characterization systems. A microscope-compatible 850-nm LED and calibrated infrared photodetector from Thorlab were used for illumination studies. The EQE measurements used a halogen white light source, a calibrated photodetector, a monochromator, an optical chopper, and a lock-in amplifier.

III. RESULTS AND DISCUSSION

A. Cell Performance

The baseline performance of the PV cells is shown in Fig. 2 under 1.06-μW/mm^2 LED irradiance at a wavelength of 850 nm. These are extremely dim irradiance conditions in comparison to AM 1.5 sunlight conditions of 1000 μW/mm^2, and represents an approximate irradiance scenario for

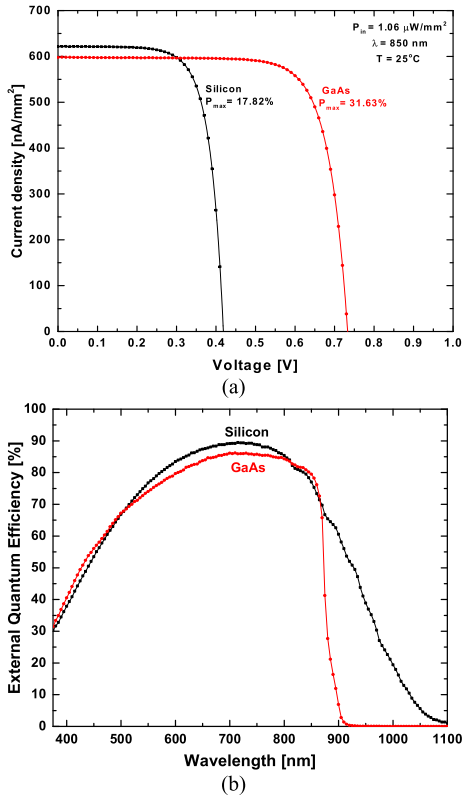

Fig. 2. Performance characteristics of silicon and GaAs photovoltaic cells. (a) Current density versus voltage under 1.06 μW/mm^2 at 850-nm wavelength and 25 °C. (b) EQE spectra.

charging. The current–voltage characteristics are shown in Fig. 2(a), demonstrating power conversion efficiency values of 17.82% for silicon PV and 31.63% for GaAs PV. The short circuit current density (J_{SC}) is similar for both silicon and GaAs, indicating similar conversion of the infrared flux to photocurrent. The EQE spectra shown in Fig. 2(b) confirm J_{SC} results, with above 80% EQE for both silicon and GaAs over the desired NIR range between 700 and 850 nm. The metal fingers used in the cell design are a primary factor limiting J_{SC} and EQE where approximately 7% of the light is reflected by metal coverage on the top surface. The primary difference in power conversion efficiency between silicon and GaAs cells is the variation in open circuit voltage (V_{OC}), which tracks the material bandgap energy. The performance of the silicon and GaAs photovoltaic cells are limited by nonradiative perimeter, surface, and Shockley–Read–Hall recombination losses [30], [31], reducing the V_{OC} below the theoretical Shockley–Queisser [35] (SQ) limit. While these PV cells demonstrate high power conversion efficiency, the SQ limit is calculated to be 32% for silicon [30] and 53% for GaAs under 660 nW/mm^{2}at 850-nm wavelength.

B. Temperature Dependence

The operating temperature of biomedical implantable devices should also be considered, where body temperature ranges between 36 °C and 37 °C, in contrast to the typical room temperature of 25 °C. The increase in operating temperature can degrade the device performance by increasing

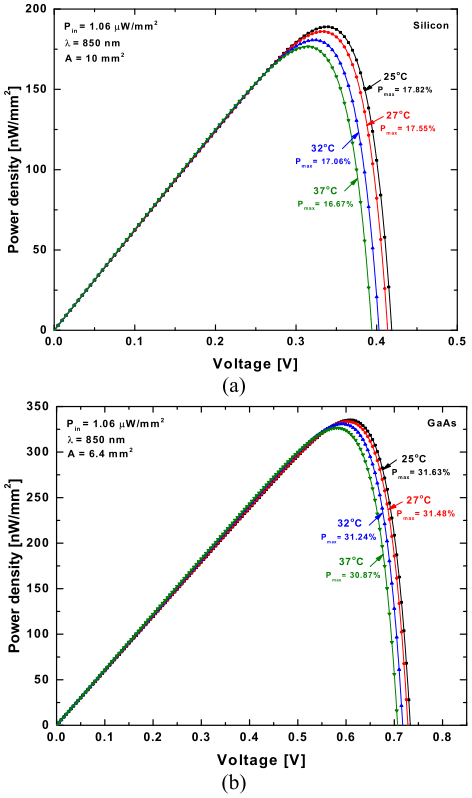

Fig. 3. Temperature dependence of power density versus voltage ranging from room temperature (25 °C) to conventional body temperature (37 °C) for (a) silicon and (b) GaAs.

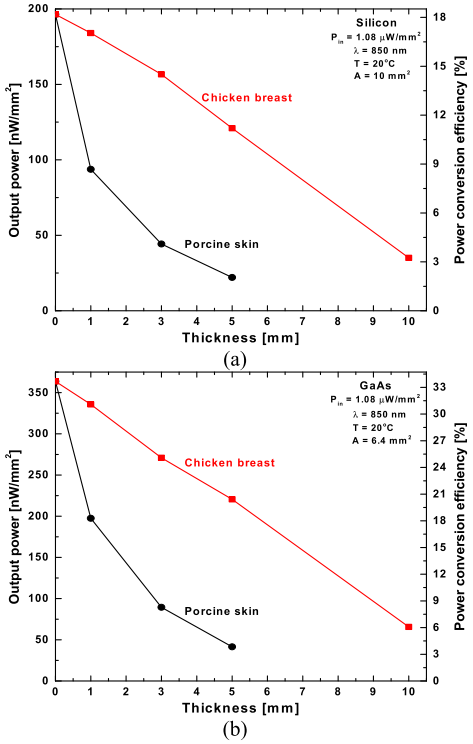

Fig. 4. Power conversion efficiency versus thickness of porcine skin and chicken breast for (a) silicon and (b) GaAs photovoltaic cells under 1.08 μW/mm^2 at 850-nm wavelength.

the thermal carrier generation and corresponding increase in reverse saturation current and decrease in open circuit voltage. The temperature dependence of the power density versus voltage is shown in Fig. 3(a) and (b) for silicon and GaAs cells, respectively, exhibiting a reduction in V_{OC} of 2.09 mV/°C for silicon and 2.23 mV/°C for GaAs. The corresponding reduction in the power conversion efficiency in this temperature range is 0.097%/°C for silicon and 0.069%/°C for GaAs. These values are consistent with theoretical temperature dependence of PV cells [36] where such minor variations in conversion efficiency can generally be neglected, i.e., room-temperature characteristics provide an adequate representation of energy harvesting performance.

C. Subcutaneous Energy Harvesting

We tested the feasibility of subcutaneous photovoltaic energy harvesting with variable thickness of tissue models via porcine skin and chicken breast to approximate properties of human skin [37]–[41] and muscle [16]. Initially, an infrared LED at 850 nm was aligned to photovoltaic cells at a fixed distance and the incident illumination density adjusted by the applied voltage to the infrared LED was scanned using a calibrated photodetector. The tissue samples with variable thickness were placed between the LED and PV cell to measure current–voltage characteristics in a through-tissue configuration. The dependence of PV cell output power density on tissue thickness is shown in Fig. 4 for irradiation under 1.08 μW/mm^{2}at a wavelength of 850 nm. The chicken breast model exhibits a near exponential dependence of power density versus thickness described by the Beer–Lambert relation [16]

$$P_{\text{out}} = P_0 e^{-\alpha d} \tag{1}$$

where P_{out} is the electrical power density produced by the cell, P_0 is the incident infrared power density, α is the attenuation coefficient, and d is the tissue thickness. An extracted attenuation coefficient of the chicken breast sample is 1.706 cm^{-1} at wavelength of 850 nm. Optical attenuation will occur via absorption and scattering, depending on the cell structure [42], and portions of blood, chromophores and pigments in the tissue. The constant attenuation coefficient for the chicken breast samples suggests a homogeneous medium, providing a good model for optical penetration into uniform soft tissue samples. The attenuation coefficient is similar to prior reports for human skin [15] of 0.37 $\pm$ 0.12 cm^{-1} and subcutaneous adipose tissue of 1.1 $\pm$ 0.03 cm^{-1} over the wavelength range between 620 and 1000 nm, and tumor samples [39] with attenuation coefficients of 3.29 $\pm$ 1.02 cm^{-1} and 4.77 $\pm$ 0.77 cm^{-1} at 789-nm wavelength. The power density dependence for harvesting through porcine skin exhibits a sharp attenuation near surface, suggesting an inhomogeneous medium. Optical transmission through human skin occurs via three primary layers [15], [16], [40]: the epidermis (100 μm thick), dermis (1–4 mm thick) and subcutaneous fat (1–6 mm thick). Attenuation in the epidermis and dermis is dominated by Mie scattering [43] via collagen fibers, where attenuation is

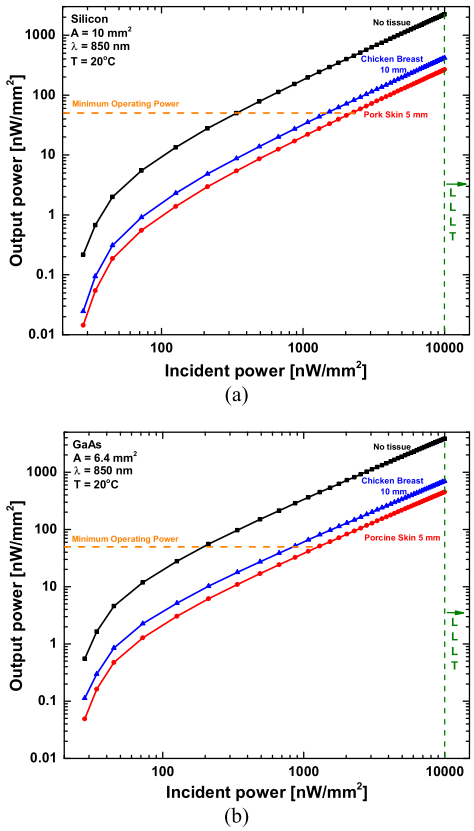

Fig. 5. Output power versus input power plots for (a) silicon and (b) GaAs photovoltaic cells through 5-mm porcine skin and 10-mm chicken breast along with minimum 50-nW/mm^2 operating power of low-power microelectronics and minimum 10-μW/mm^2 LLLT.

reduced for latter propagation in fatty tissue. The porcine skin model therefore represents a good approximation to transmission through skin with high density of collagen fibers [37] in the dermis compared to human skin, and represents a worst case scenario for IR attenuation.

The dependence of output power density versus input irradiance is shown in Fig. 5 for silicon and GaAs samples of 5-mm porcine skin and 10-mm chicken breast. Above irradiance of approximately 100 nW/mm^2, the harvesting efficiency is approximately constant, corresponding to the linear relationship on the log-log scale of Fig. 5. The energy harvesting efficiency decreases below irradiance of 100 nW/mm^2, attributed to the regime where dark current density in the PV cells approaches the photo-generated current. The approximate requirement to power millimeter-scale systems is 50 nW/mm^2[22], which is demonstrated for all tissue samples in Fig. 5 for irradiance above 2.3 μW/mm^2 for silicon and 1.3 μW/mm^2 for GaAs. This irradiance condition is within an acceptable range of operation, and is below the typical minimum power density of 10 μW/mm^2 that is safely used in low-level laser therapy (LLLT) for medical treatments [34] and produces a slight rise (below 0.5 °C) in the temperature of tissue/PV with negligible temperature degradations for PVs [12].

We studied a more complex energy harvesting scenario using NIR transmission through a previously dissected mouse to include complex combinations of hair, skin, bone, muscle, and organs. The dissected mouse sample was placed between the LED and PV cell for seven specific sections of the mouse sample, as shown in Fig. 6. Energy harvesting was measured using LED irradiance from above, with PV cells placed beneath the mouse. PV performance for the seven locations is summarized in Table II. LED irradiation at 134 μW/mm^2 (within the typical range of LLLT between 10 μW/mm^2 and 10 mW/mm^2) demonstrated stable harvesting capabilities at all seven locations. The ability to demonstrate energy harvesting at these locations, particularly point 7, which is a 15-mm-thick thorax region with high tissue density, shows great promise for infrared power transfer.

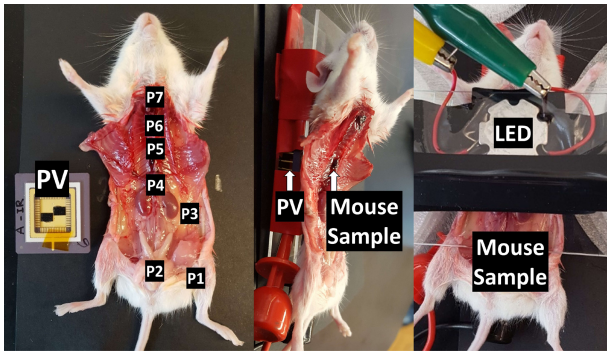

Fig. 6. Photograph of dissected mouse and mounted PV cells used to measure NIR energy harvesting.

TABLE II
PARAMETERS MEASURED AT VARIOUS LOCATIONS ON THE SAMPLE

#	Thickness [mm]	Input power [μW/mm^2]	GaAs		Silicon	
			Output power [μW/mm^2]	Efficiency [%]	Output power [μW/mm^2]	Efficiency [%]
Point 1	7	134	5.12	3.82	2.82	2.1
Point 2	10	134	2.74	2.05	1.48	1.1
Point 3	4	134	12.24	9.13	7.75	5.79
Point 4	6	134	8.04	6.00	4.85	3.62
Point 5	10	134	3.4	2.53	2.07	1.54
Point 6	12	134	1.19	0.89	0.82	0.61
Point 7	15	134	0.29	0.21	0.17	0.12

Our silicon and GaAs cells demonstrate the ability to power biologically implanted millimeter-scale systems under low NIR irradiance conditions (approximately 1 μW/mm^2). Beyond the power generated by the PV cells, the implantable system will require an interface to directly power the system or to charge a battery. We have previously demonstrated that energy harvesting circuitry can exceed 78% at similar scale and low-flux conditions [44] using a series/parallel PV network to match the charging voltage required for a battery without the need for voltage upconversion. Further improvements in the cell structure will require the encapsulation of photovoltaic cells with biocompatible and transparent polymer packaging materials, such as poly(methyl methacrylate) [45] and polydimethylsiloxane [33], [46] or glass [47] for long-term stability to reduce the toxicity concern of arsenic compounds.

IV. CONCLUSION

Our results demonstrate that external infrared energy harvesting from ambient sources or intentional irradiation is suf-

ficient to power millimeter-scale sensor systems utilizing silicon or GaAs PV cells that are specifically designed and optimized for energy harvesting in the NIR transparency window for biological tissue. Sufficient power generation is achieved for perpetual operation of millimeter-scale systems for implant depth of at least 15 mm, including hair/skin/muscle/bone under NIR illumination at 850 nm.

REFERENCES

[1] A. Cadei, A. Dionisi, E. Sardini, and M. Serpelloni, "Kinetic and thermal energy harvesters for implantable medical devices and biomedical autonomous sensors," *Meas. Sci. Technol.*, vol. 25, no. 1, p. 012003, 2013.

[2] R. Venkatasubramanian, E. Siivola, T. Colpitts, and B. O'Quinn, "Thin-film thermoelectric devices with high room-temperature figures of merit," *Nature*, vol. 413, no. 6856, pp. 597–602, 2001.

[3] Y. Yang, X.-J. Wei, and J. Liu, "Suitability of a thermoelectric power generator for implantable medical electronic devices," *J. Phys. D, Appl. Phys.*, vol. 40, no. 18, p. 5790, 2007.

[4] S. R. Platt, S. Farritor, K. Garvin, and H. Haider, "The use of piezoelectric ceramics for electric power generation within orthopedic implants," *IEEE/ASME Trans. Mechatronics*, vol. 10, no. 4, pp. 455–461, Aug. 2005.

[5] S. Almouahed, M. Gouriou, C. Hamitouche, E. Stindel, and C. Roux, "Self-powered instrumented knee implant for early detection of postoperative complications," in *Proc. Annu. Int. Conf. IEEE Eng. Med. Biol. Soc. (EMBC)*, Aug. 2010, pp. 5121–5124.

[6] B. E. Lewandowski, K. L. Kilgore, and K. J. Gustafson, "Design considerations for an implantable, muscle powered piezoelectric system for generating electrical power," *Ann. Biomed. Eng.*, vol. 35, no. 4, pp. 631–641, 2007.

[7] J.-D. Kim, C. Sun, and I.-S. Suh, "A proposal on wireless power transfer for medical implantable applications based on reviews," in *Proc. IEEE Wireless Power Transf. Conf. (WPTC)*, May 2014, pp. 166–169.

[8] S. B. Lee, H.-M. Lee, M. Kiani, U.-M. Jow, and M. Ghovanloo, "An inductively powered scalable 32-channel wireless neural recording system-on-a-chip for neuroscience applications," *IEEE Trans. Biomed. Circuits Syst.*, vol. 4, no. 6, pp. 360–371, Dec. 2010.

[9] R. Bashirullah, "Wireless implants," *IEEE Microw. Mag.*, vol. 11, no. 7, pp. S14–S23, Dec. 2010.

[10] R.-F. Xue, K.-W. Cheng, and M. Je, "High-efficiency wireless power transfer for biomedical implants by optimal resonant load transformation," *IEEE Trans. Circuits Syst. I, Reg. Papers*, vol. 60, no. 4, pp. 867–874, Apr. 2013.

[11] A. K. RamRakhyani, S. Mirabbasi, and M. Chiao, "Design and optimization of resonance-based efficient wireless power delivery systems for biomedical implants," *IEEE Trans. Biomed. Circuits Syst.*, vol. 5, no. 1, pp. 48–63, Feb. 2011.

[12] K. Goto, T. Nakagawa, O. Nakamura, and S. Kawata, "An implantable power supply with an optically rechargeable lithium battery," *IEEE Trans. Biomed. Eng.*, vol. 48, no. 7, pp. 830–833, Jul. 2001.

[13] K. Murakawa, M. Kobayashi, O. Nakamura, and S. Kawata, "A wireless near-infrared energy system for medical implants," *IEEE Eng. Med. Biol. Mag.*, vol. 18, no. 6, pp. 70–72, Nov./Dec. 1999.

[14] S. Ayazian, V. A. Akhavan, E. Soenen, and A. Hassibi, "A photovoltaic-driven and energy-autonomous CMOS implantable sensor," *IEEE Trans. Biomed. Circuits Syst.*, vol. 6, no. 4, pp. 336–343, Aug. 2012.

[15] A. N. Bashkatov, E. A. Genina, V. I. Kochubey, and V. V. Tuchin, "Optical properties of human skin, subcutaneous and mucous tissues in the wavelength range from 400 to 2000 nm," *J. Phys. D, Appl. Phys.*, vol. 38, no. 15, p. 2543, 2005.

[16] L. A. Sordillo, Y. Pu, S. Pratavieira, Y. Budansky, and R. R. Alfano, "Deep optical imaging of tissue using the second and third near-infrared spectral windows," *J. Biomed. Opt.*, vol. 19, no. 5, p. 056004, 2014.

[17] A. M. Smith, M. C. Mancini, and S. Nie, "Second window for *in vivo* imaging," *Nature Nanotechnol*, vol. 4, no. 11, pp. 710–711, 2009.

[18] M. C. Frost and M. E. Meyerhoff, "Implantable chemical sensors for real-time clinical monitoring: Progress and challenges," *Current Opinion Chem. Biol.*, vol. 6, no. 5, pp. 633–641, 2002.

[19] R. K. Meruva and M. E. Meyerhoff, "Catheter-type sensor for potentiometric monitoring of oxygen, pH and carbon dioxide," *Biosens. Bioelectron.*, vol. 13, no. 2, pp. 201–212, 1998.

[20] D. S. Bindra *et al.*, "Design and *in vitro* studies of a needle-type glucose sensor for subcutaneous monitoring," *Anal. Chem.*, vol. 63, no. 17, pp. 1692–1696, 1991.

[21] X. Chen, N. Matsumoto, Y. Hu, and G. S. Wilson, "Electrochemically mediated electrodeposition/electropolymerization to yield a glucose microbiosensor with improved characteristics," *Anal. Chem.*, vol. 74, no. 2, pp. 368–372, 2002.

[22] Y. Lee *et al.*, "A modular 1 mm^3 die-stacked sensing platform with low power I^2C inter-die communication and multi-modal energy harvesting," *IEEE J. Solid-State Circuits*, vol. 48, no. 1, pp. 229–243, Jan. 2013.

[23] S. Oh *et al.*, "A dual-slope capacitance-to-digital converter integrated in an implantable pressure-sensing system," *IEEE J. Solid-State Circuits*, vol. 50, no. 7, pp. 1581–1591, Jul. 2015.

[24] S. Jeong, Z. Foo. Y. Lee, J.-Y. Sim, D. Blaauw, and D. Sylvester, "A fully-integrated 71 nW CMOS temperature sensor for low power wireless sensor nodes," *IEEE J. Solid-State Circuits*, vol. 49, no. 8, pp. 1682–1693, Aug. 2014.

[25] G. Kim *et al.*, "A millimeter-scale wireless imaging system with continuous motion detection and energy harvesting," in *Symp. VLSI Circuits Dig. Tech. Papers*, Jun. 2014, pp. 1–2.

[26] Y. Lee, D. Blaauw, and D. Sylvester, "Ultralow power circuit design for wireless sensor nodes for structural health monitoring," *Proc. IEEE*, vol. 104, no. 8, pp. 1529–1546, Aug. 2016.

[27] M. Catrysse, B. Hermans, and R. Puers, "An inductive power system with integrated bi-directional data-transmission," *Sens. Actuators A, Phys.*, vol. 115, nos. 2–3, pp. 221–229, Sep. 2004.

[28] B. M. Kayes *et al.*, "27.6% Conversion efficiency, a new record for single-junction solar cells under 1 sun illumination," in *Proc. 37th IEEE Photovolt. Specialists Conf. (PVSC)*, Jun. 2011, pp. 000004–000008.

[29] J. Zhao, A. Wang, M. A. Green, and F. Ferrazza, "19.8% efficient 'honeycomb' textured multicrystalline and 24.4% monocrystalline silicon solar cells," *Appl. Phys. Lett.*, vol. 73, no. 14, pp. 1991–1993, 1998.

[30] E. Moon, D. Blaauw, and J. D. Phillips, "Small-area Si photovoltaics for low-flux infrared energy harvesting," *IEEE Trans. Electron Devices*, vol. 64, no. 1, pp. 15–20, Jan. 2017.

[31] A. S. Teran *et al.*, "Energy harvesting for GaAs photovoltaics under low-flux indoor lighting conditions," *IEEE Trans. Electron Devices*, vol. 63, no. 7, pp. 2820–2825, Jul. 2016.

[32] K. Rühle, M. Freunek, L. M. Reindl, and M. Kasemann, "Designing photovoltaic cells for indoor energy harvesting systems," in *Proc. 9th Int. Multi-Conf. Syst., Signals Devices (SSD)*, Mar. 2012, pp. 1–5.

[33] K. Song *et al.*, "Subdermal flexible solar cell arrays for powering medical electronic implants," *Adv. Healthcare Mater.*, vol. 5, no. 13, pp. 1572–1580, 2016.

[34] H. Chung, T. Dai, S. K. Sharma, Y.-Y. Huang, J. D. Carroll, and M. R. Hamblin, "The nuts and bolts of low-level laser (light) therapy," *Ann. Biomed. Eng.*, vol. 40, no. 2, pp. 516–533, 2012.

[35] W. Shockley and H. J. Queisser, "Detailed balance limit of efficiency of $p-n$ junction solar cells," *J. Appl. Phys.*, vol. 32, no. 3, pp. 510–519, 1961.

[36] J. C. C. Fan, "Theoretical temperature dependence of solar cell parameters," *Solar cells*, vol. 17, nos. 2–3, pp. 309–315, 1986.

[37] N. J. Vardaxis, T. A. Brans, M. E. Boon, R. W. Kreis, and L. M. Marres, "Confocal laser scanning microscopy of porcine skin: Implications for human wound healing studies," *J. Anatomy*, vol. 190, no. 4, pp. 601–611, 1997.

[38] E. Zamora-Rojas, B. Aernouts, A. Garrido-Varo, D. Pérez-Marín, J. E. Guerrero-Ginel, and W. Saeys, "Double integrating sphere measurements for estimating optical properties of pig subcutaneous adipose tissue," *Innov. Food Sci. Emerg. Technol.*, vol. 19, pp. 218–226, Jul. 2013.

[39] M. R. Arnfield, R. P. Mathew, J. Tulip, and M. S. McPhee, "Analysis of tissue optical coefficients using an approximate equation valid for comparable absorption and scattering," *Phys. Med. Biol.*, vol. 37, no. 6, p. 1219, 1992.

[40] Y. Du, X. H. Hu, M. Cariveau, X. Ma, G. W. Kalmus, and J. Q. Lu, "Optical properties of porcine skin dermis between 900 nm and 1500 nm," *Phys. Med. Biol.*, vol. 46, no. 1, p. 167, 2001.

[41] W. Meyer, R. Schwarz, and K. Neurand, "The skin of domestic mammals as a model for the human skin, with special reference to the domestic pig1," in *Skin-Drug Application and Evaluation of Environmental Hazards*. Basel, Switzerland: Karger Publishers, 1978, pp. 39–52.

[42] S. L. Jacques, "Optical properties of biological tissues: A review," *Phys. Med. Biol.*, vol. 58, no. 11, p. R37, 2013.

[43] I. S. Saidi, S. L. Jacques, and F. K. Tittel, "Mie and Rayleigh modeling of visible-light scattering in neonatal skin," *Appl. Opt.*, vol. 34, no. 31, pp. 7410–7418, 1995.
[44] I. Lee, W. Lim, A. Teran, J. Phillips, D. Sylvester, and D. Blaauw, "A >78%-efficient light harvester over 100-to-100klux with reconfigurable PV-cell network and MPPT circuit," in *IEEE Int. Solid-State Circuits Conf. (ISSCC) Dig. Tech. Papers*, Jan. 2016, pp. 370–371.
[45] S. J. Kim *et al.*, "The potential role of polymethyl methacrylate as a new packaging material for the implantable medical device in the bladder," *BioMed Res. Int.*, vol. 2015, Feb. 2015, Art. no. 852456.
[46] S. L. Peterson, A. McDonald, P. L. Gourley, and D. Y. Sasaki, "Poly(dimethylsiloxane) thin films as biocompatible coatings for microfluidic devices: Cell culture and flow studies with glial cells," *J. Biomed. Mater. Res. A*, vol. 72, no. 1, pp. 10–18, 2005.
[47] J. H.-C. Chang, Y. Liu, and Y.-C. Tai, "Long term glass-encapsulated packaging for implant electronics," in *Proc. IEEE 27th Int. Conf. Micro Elect. Mech. Syst. (MEMS)*, Jan. 2014, pp. 1127–1130.

Eunseong Moon (S'16) received the B.S. degree in electrical engineering from Chung-Ang University, Seoul, South Korea, in 2012, and the M.S. degree in electrical engineering from the University of Michigan, Ann Arbor, MI, USA, in 2015, where he is currently pursuing the Ph.D. degree.

His current research interests include photovoltaic energy harvesting for millimeter-scale systems.

David Blaauw (SM'07–F'12) received the B.S. degree in physics and computer science from Duke University, Durham, NC, USA, in 1986, and the Ph.D. degree in computer science from the University of Illinois at Urbana–Champaign, Champaign, IL, USA, in 1991.

Since 2001, he has been a Faculty Member with the University of Michigan, Ann Arbor, MI, USA, where he is currently a Professor.

Jamie D. Phillips (M'01–SM'06) received the B.S., M.S., and Ph.D. degrees in electrical engineering from the University of Michigan, Ann Arbor, MI, USA.

He has been a Faculty Member with the University of Michigan since 2002, where he is currently an Arthur F. Thurnau Professor. His current research interests include compound semiconductor and oxide-based materials for optoelectronics and electronics.